

An Electrostatic Cloud Droplet Probe

CHARLES E. ABBOTT, JAMES E. DYE AND J. DOYNE SARTOR

National Center for Atmospheric Research,¹ Boulder, Colo. 80302

(Manuscript received 6 April 1972, in revised form 6 July 1972)

ABSTRACT

An electrostatic cloud droplet sizing device (electrostatic disdrometer) originally developed by Keily and Millen has been tested, modified extensively, and calibrated in our laboratory. The investigations have shown that soon after entry into the probe orifice, the incoming droplet is broken into many fragments. These fragments impact and splash on an electrode raised to a 510 V potential. Measured pulses for a given droplet size give a reproducible calibration curve.

Airborne tests of the probe have shown it to operate reliably with minimal maintenance. Comparisons were made between values of the liquid water content measured by the electrostatic disdrometer and by the Johnson-Williams hot-wire, liquid-water-content meter and between the droplet size distributions measured by the disdrometer and by impaction slide replicas. The comparisons were satisfactory within the limits of instrument measuring and sampling errors and actual variations in the droplets spectra resulting from the separation of the instruments on the aircraft during the tests.

1. Introduction

An instrument for measuring cloud-droplet size by electronically sensing the removal of charge from an electrified probe by the impacting droplets was designed and developed by Keily and Millen (1960) for the Air Force Cambridge Research Laboratories (AFCRL). Although laboratory calibrations of the instrument gave a reproducible straight line relationship between the electronic pulse amplitude and the approximate square of the radius of the droplets, airborne tests appeared to give questionable or possibly spurious results.

Because of this instrument's potential for obtaining automatic and easily processed droplet size distributions with rapid repetition rates, we obtained a prototype from R. M. Cunningham (AFCRL) with the intention of verifying Keily and Millen's early laboratory results and investigating the use of solid-state electronics to identify sources of microphonics and spurious signals which occur during airborne operation of the instrument.

We performed laboratory experiments to determine the source of the pulses detected at the electrode and made some changes in the internal geometry to improve the performance. A transistorized amplifier was substituted for the original tube version to improve reliability and reduce microphonics. A pulse-height analyzer was constructed to permit rapid analysis of the data and has been used to obtain continuous droplet distributions with 0.5-sec resolution.

Several flight tests were made in warm clouds to compare the data obtained with the new instrument

with those obtained simultaneously with a Johnson-Williams hot-wire device (liquid water content) and with impactor slides (droplet distributions). The comparisons were satisfactory within the limits of measuring and sampling errors of the Johnson-Williams liquid-water-content meter and the impactor slides and the actual variations in the droplet spectra resulting from the separation of the instruments.

2. The instrument

Basically, the probe operates as follows:

Air, containing droplets to be measured, is drawn through an orifice at near sonic velocities by a vacuum pump. Inside the orifice each droplet breaks up into a group of smaller droplets. The group of droplets subsequently strikes a metallic electrode aligned with the

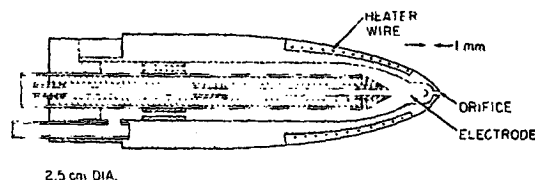


FIG. 1. Schematic diagram of the tip of the present model of the electrostatic disdrometer.

¹The National Center for Atmospheric Research is sponsored by the National Science Foundation.

axis of the inlet hole and raised to a high potential with respect to the surrounding housing. During the short time the group of droplets are impacting on the electrode, a voltage pulse is observed that is proportional in amplitude to the original droplet size.

The tip of the electrode and the housing, as it is now constructed, are shown in Fig. 1. The tip's outer shape is the forward half of an ellipsoid of revolution with a fineness ratio of 4 and a minor axis of 2.5 cm. Behind the portion shown in Fig. 1 is a cylindrical section 15 cm long containing a transistorized preamplifier. The entire assembly is supported away from the aircraft by a streamlined strut 30 cm long on the NCAR Queen Air (Fig. 2) and by a nose boom 75 cm long on "The Explorer," a Schweitzer 2-32 sailplane owned by NOAA but instrumented and operated by NCAR (Fig. 3).

3. Laboratory tests and calibration

During initial attempts to calibrate a probe constructed according to the description given by Keily and Millen we observed pulse amplitudes somewhat dependent on drop radius but with large variations, even though the sizes of the input droplets were well controlled and quite uniform. Also, the rise time of the pulse (3.5×10^{-5} sec) seemed too long in terms of the time required for a single droplet to pass from the outlet of the orifice to the electrode. A transit time of only 4.25×10^{-6} sec is calculated using the measured average velocity through the inlet hole. The time for breakup after hitting the electrode would be even less. The possibility remained that the droplet was being broken up or severely elongated before hitting the electrode or that a spurious signal was produced in some unknown way. To resolve this question we undertook extensive tests to determine the origin of the pulse.

Keily and Millen were unable to visually observe the droplets once they entered the inlet hole, but by coating the sensing electrode tip with ink, they determined that the droplets did strike the electrode. Similarly, we

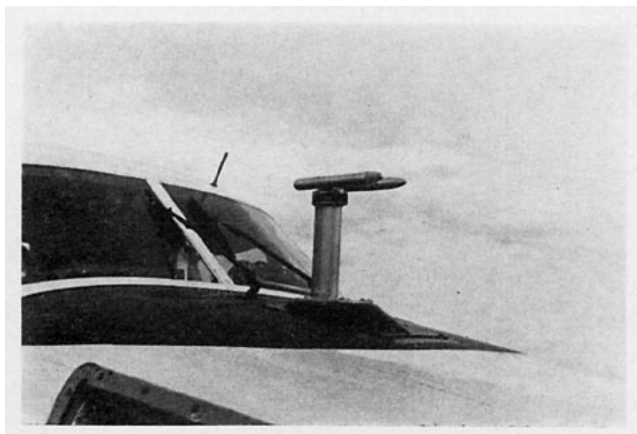


FIG. 2. Photograph of two electrostatic disdrometers mounted on an NCAR Queen Air. The probe on the left is a heated model, and the one on the right an unheated model.



FIG. 3. Photograph of the disdrometer mounted on a 75 cm long boom on "The Explorer" sailplane.

reconfirmed that the droplets physically were hitting the sensor properly. We also coated the sensing electrode tip with a thin layer of nonconducting wax, thus eliminating all charge transfer paths but not removing mechanical shocks from the droplets striking the probe. In this case, pulses from the electrode were not produced with the electrode raised to the operating potential of 510 V. From this we concluded that, with droplets striking the sensing electrode, the pulses were not due to mechanical excitation but to charge transfer from the charged electrode to the droplets.

Since the droplet's trajectory and shape within the cavity seemed of prime importance, a test probe was constructed with viewing ports in the probe body normal to the electrode tip. The electrode pulse was displayed on a Hewlett Packard Model 175 A oscilloscope, and the sweep start pulse from the oscilloscope was applied to a General Radio Type 1539-A Stroboslave. When the amplitude of the electrode voltage pulse exceeded the oscilloscope triggering level, the Stroboslave flashed. Adjustment of the triggering level allowed us to flash the Stroboslave at any time during the rise of the electrode pulse, and by using a system of dark field illumination the droplet characteristics and position within the probe could be correlated with the voltage pulse. Uniform droplets of each desired size were produced by a vibrating reed similar to that described by Harris (1964). Size was determined by observing the droplets with a synchronized strobe flash and a microscope.

Fig. 4 is a photograph of the event described with a typical resulting electrode voltage change shown in Fig. 5. To obtain the photograph for Fig. 4, the strobe flash was delayed and was triggered when the pulse reached one-half its expected amplitude. In these tests the pulse had a $35\text{-}\mu\text{sec}$ rise time. The airflow and droplet motion is from left to right. The electrode, barely visible as the dark object to the right of the bright vertical band, has a flattened tip rather than a

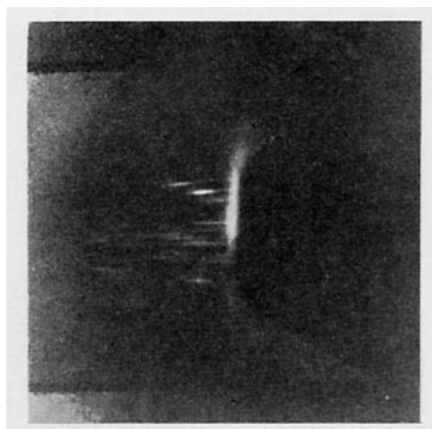


FIG. 4. Photograph showing the fragments of a 28- μm radius droplet approaching the electrode (the dark flat object on the right). The bright area immediately in front of the electrode appears to be an atomized mist caused by further breakup of the fragments.

hemispherical one constructed later and depicted in Fig. 1, and the entry orifice is longer. The photographs, represented by Fig. 4, showed that the original droplet was being shattered while still in the inlet hole and that the resulting fragments were crossing the high field region toward the electrode. The duration of the strobe flash was 3 μsec , but the motion of the droplet fragments caused streaking of the photographic images. From the duration of the flash and the length of the streaks, the fragment velocity was estimated to be 10^4 cm sec^{-1} . When the input droplet had a radius of 25 μm the fragments numbered between 30 and 40. The number was not uniform for successive droplets of the same size nor were the fragments of one drop equal in size. If a 25- μm droplet was broken into 40 equal sized fragments, the fragment radius would be 7.3 μm . Both the position of the droplet source external to the probe and the pressure drop across the orifice affected these quantities. When the fragments strike the electrode and the strobe flash is set at the pulse threshold, it illuminates what appears to be an area of atomized mist immediately in front of the electrode. An occasional bright flash can be seen, but otherwise it has not been possible to identify individual particles. Splashing of the fragments with further breakup is probably occurring.

When the strobe was triggered so that the event was illuminated at the peak of the voltage pulse all of the fragments had reached the electrode. Thus, the rise time of the pulse is apparently the result of the arrival and splashing of the droplet fragments. The decay of the pulse is determined mainly by the amplifier input time constant, which is larger than the duration of the event.

With the stroboscope triggering arrangement described above we were unable to observe the earlier stages of the event and the original droplet shattering. To observe the earlier stages, the droplets were positively charged as they were produced by the generator.

This charge caused a change in voltage on the electrode as the drop crossed the gap inside the probe. The voltage amplitude change resulting from a charged droplet when no potential is applied to the electrode is shown in Fig. 6. The duration of the rise of the changing potential is a measure of the time required for all fragments to traverse the gap and strike the electrode. It was possible to decrease the rise time of the pulse to 20 μsec by decreasing the electrode spacing although none of the waveforms observed were as rapid as those characteristic of a sparking discharge (<1 nsec) as reported by Miller *et al.* (1965), indicating that spark discharge does not occur. The uniform pulse amplitudes recorded using this technique indicated that the source of uniform droplets was very stable and that the random variations in fragment breakup before or as they strike the electrode are responsible for the observed variations in pulse amplitude during calibration. If the total charge on the original droplet were placed on the electrode, the voltage would have reached a peak and then remained constant. However, some of the charge is carried away by the small particles as they leave the electrode, and it is at this point that variations in pulse shape are seen in Fig. 6. When the charge on the droplet was kept constant and the potential applied to the electrode was gradually increased from zero to the usual operating voltage, the normally observed pulse of larger amplitude and opposite polarity was seen. The timing of this pulse was coincident with the region on Fig. 6 in which the variations are observed and the point at which the particles are hitting and leaving the electrode.

Occasionally the fragments approaching the electrode were in two distinct groups with the trailing fragments having the larger radii. When two groups of fragments were observed, double peaked pulses, which Keily (1964) reported occasionally observing, were seen on the oscilloscope.

To determine the effects of large electrodes, a test probe was constructed with an electrode 1 cm in diameter. The inlet-hole diameter was 1 mm, and the

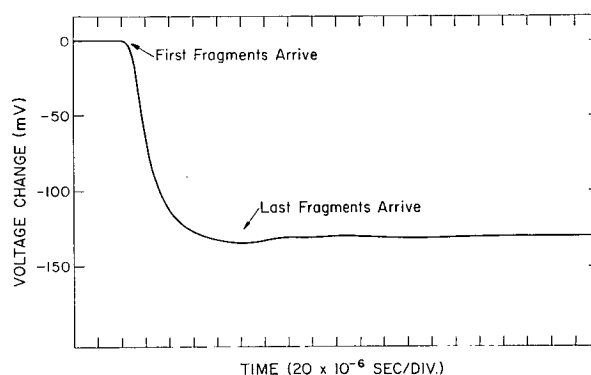


FIG. 5. Voltage change observed for a 22- μm radius droplet approaching and impacting on the electrode raised to a potential of 510 V.

gap was 1 mm. Attempts to calibrate the probe with this geometry revealed erratic operation. The pulse amplitudes for the same input-drop radius varied by as much as a factor of 10, and a discontinuity in the trailing edge of the waveform was evident. The charge on the electrode increased after reaching its peak negative value (Fig. 5). From examination of the electrode with stroboscopic light at this time it could be seen that after leaving the electrode some of the particles were falling back to the surface about 3–4 mm away from the initial point of impact. Therefore, the discontinuity is probably caused by the return of some of the charged fragments to the electrode.

With the previous observations as a guide, a probe of the dimensions shown in Fig. 1 was constructed and calibrated. The major differences from those used by Keily are a shorter inlet hole, a smaller separation between housing and electrode, and a hemispherical rather than a flat electrode tip to eliminate irregularities in the field at the surface of the electrode. The breakup into fragments of the original droplet was more regular with the shallow hole. The shallow hole and smaller separation of the electrode from the housing lessened the possibility of fragments striking the walls or missing the electrode since the breakup occurred near the exit of the hole. The length of the hole was decreased from 4.5 mm to 1 mm. The hemispherical electrode tip presented a good target area for the fragments but still allowed the particles to be swept away instead of falling back and collecting on the surface.

The probe electronics presently in use consist of two integrated circuits. The first is a unity gain voltage follower to provide current amplification of the electrode pulses. It has an input resistance of $2.5 \times 10^6 \Omega$ and an input capacitance of $6 \times 10^{-2} \text{ F}$. The second amplifier has a voltage gain of 27 and produces output pulses of sufficient amplitude to trigger the pulse height analyzer located inside the aircraft.

A calibration of the probe with the present geometry and electronics is shown in Fig. 7. The radius r (cm) of the uniformly produced droplets was determined by observing the droplets with a microscope and stroboscopic illumination just before they entered the orifice.

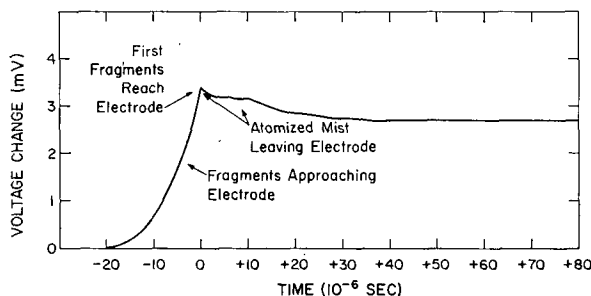


FIG. 6. Observed voltage change for a positively charged droplet approaching and impacting on the electrode when no potential is applied to the electrode.

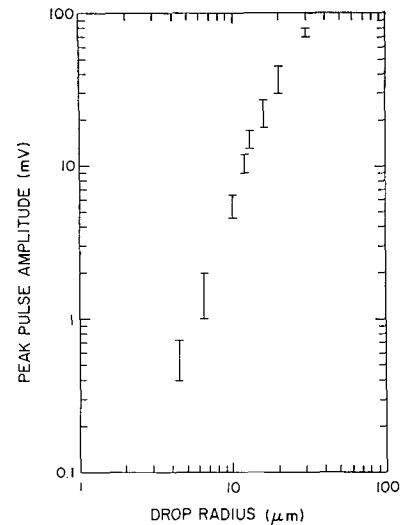


FIG. 7. Calibration curve of the electrostatic disdrometer with the geometry shown in Fig. 1.

The error bars represent the minimum and maximum pulse amplitudes recorded for approximately 100 successive input droplets. The change in charge observed ($1.6 \times 10^{-7} r^2 \text{ C}$ for droplets $> 10 \mu\text{m}$) is much larger than the charge which droplets have been found to carry in the atmosphere. The value of $-4.8 \times 10^{-10} r^2 \text{ C}$ reported by Krasnogorskaya (1969) and $-5.7 \times 10^{-10} r^2 \text{ C}$ by Colgate and Romero (1970) is typical of charge distributions measured in electrified clouds by other investigators.

4. Data recording

The pulse amplitudes shown in Fig. 7 are sized and counted electronically by a 10-channel pulse height analyzer to obtain a histogram of the droplet distribution.

Parallel-connected voltage comparators are triggered by the incoming pulse with all lower channels inhibited by the highest channel triggered, which represents the peak pulse amplitude. After the pulses are sized, analog storage elements in each channel total the counts for 0.5 sec. The accumulated count is then transferred to hold circuits, and the storage elements are reset to begin accumulating counts for the next 0.5 sec. During this time the hold circuits are commutated and applied to a logarithmic amplifier. The final output signal is a histogram of the pulse amplitudes for the previous 0.5 sec. Fig. 8 is an example of a series of histograms obtained from a typical flight through a cloud. The negative pulse indicates the start of each new histogram. The present channel interval data format is shown in Table 1.

On the NCAR Queen Air the data from the pulse height analyzer are recorded on magnetic tape with the NCAR Research Aviation Facility's ARIS (Aircraft

CLOUD PHYSICS

26FEB71 14:24:15EST

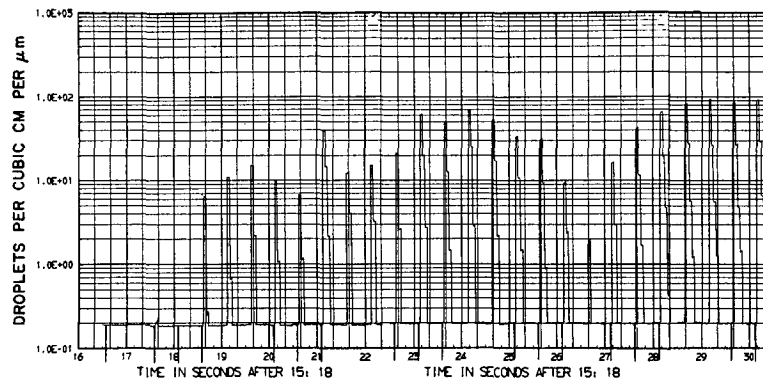


FIG. 8. A sample of continuous droplet distribution measurements (summed every 0.5 sec) obtained by the electrostatic disdrometer during a cloud traverse near Miami, Fla., at 1980 m on the NCAR Queen Air. The channels are $3\ \mu\text{m}$ wide with the first channel starting from the left at $4\ \mu\text{m}$ radius.

Recording Instrumentation System) and then processed directly by computer. Data collected on "The Explorer" sailplane are telemetered to the ground, recorded on magnetic tape, and then processed by computer. An example of processed data is shown in Fig. 9. The volume swept out by the inlet hole of the probe during the sample time and the cloud droplet count are used to determine droplet density. At typical Queen Air aircraft speeds of $75\ \text{m sec}^{-1}$ with a hole $250\ \mu\text{m}$ in diameter and a 0.5-sec sampling period, the maximum density is limited to $400\ \text{droplets cm}^{-3}\ \mu\text{m}^{-1}$ in each channel. The sailplane speed is typically $35\ \text{m sec}^{-1}$. The logarithmic amplifier provides a three-decade range so that the minimum count detectable is $0.4\ \text{droplets cm}^{-3}\ \mu\text{m}^{-1}$ per 0.5 sec. This minimum count limit could be improved by enlarging the inlet hole to sample a larger volume, but the present opening appears to be close to optimum for this instrument in the cloud-droplet size range. If we examine the case for high droplet concentrations, i.e., $1000\ \text{droplets cm}^{-3}$, the count rate on the Queen Air at $75\ \text{m sec}^{-1}$ is about $3750\ \text{counts sec}^{-1}$, or if the droplets are equally spaced in time a droplet is counted each $267\ \mu\text{sec}$. With the present electronics the pulse duration is $50\ \mu\text{sec}$. Thus, even for $1000\ \text{droplets cm}^{-3}$ the likelihood of loss by

coincidence is low. A lower threshold for the droplet concentrations in the last four channels has been achieved without losing spatial resolution by incrementing the 0.5-sec data for eight intervals and resetting these channels every 4 sec instead of every 0.5 sec. The minimum detectable count in each of these channels is then $0.03\ \text{droplets cm}^{-3}\ \mu\text{m}^{-1}$ over a $300\ \text{m}$ path at $75\ \text{m sec}^{-1}$.

5. Collection efficiency

The collection efficiency of the probe has been determined theoretically by Drake *et al.* (1972), assuming the probe to be an ellipsoid of revolution with a sampling

TABLE 1. Data format of the electrostatic disdrometer.

Channel no.	Radius interval (μm)	Channel width (μm)
1	4.0—5.5	1.5
2	5.5—7.0	1.5
3	7.0—8.5	1.5
4	8.5—10.0	1.5
5	10.0—11.5	1.5
6	11.5—13.0	1.5
7	13.0—16.0	3
8	16.0—19.0	3
9	19.0—22.0	3
10	>22.0	—

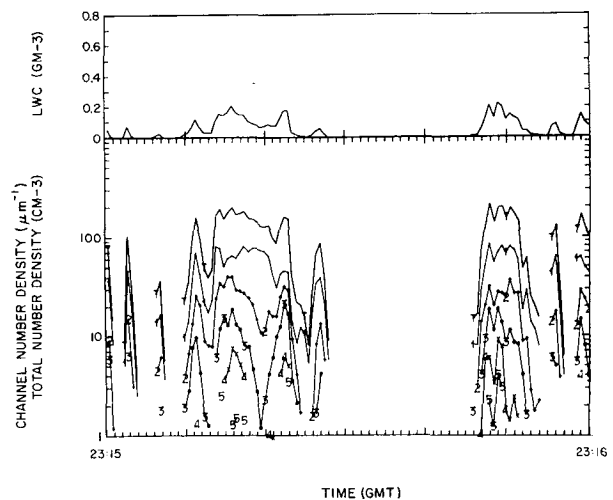


FIG. 9. A sample of processed data obtained by the electrostatic disdrometer on "The Explorer" sailplane on 15 July 1971 at $3600\ \text{m}$ in broken stratocumulus clouds over Ft. Morgan, Colo. The T denotes total droplet concentration and the 1, 2, 3, 4, and 5 denote the concentration per μm in the radius intervals 4-5.5, 5.5-7, 7-8.5, 8.5-10, and 10-11.5 μm , respectively. The liquid water content obtained by integration of the disdrometer data is shown at the top of the figure.

hole at the forward stagnation point with steady, axisymmetric, irrotational and incompressible flow at standard temperature and pressure. A plot of collection efficiency vs droplet radius for various aircraft speeds is shown in Fig. 10. There is an enhancement in droplet count for small droplets and lower speeds because the flow through the probe is greater than the volume intercepted by the orifice. The calculated collection efficiencies are considered to be quite accurate because exact solutions were obtained for the flow field resulting from axial symmetry and the mathematically describable shape of the probe. The calculated collection efficiency of the probe is unity for droplets $>4 \mu\text{m}$ in radius (the minimum size counted with the probe) with a maximum error of $\pm 5\%$ at typical aircraft speeds $\geq 67 \text{ m sec}^{-1}$. Keily and Millen (1960) also calculated collection efficiencies for their probe which are similar to the present calculations. Since the fineness ratio of the two probes is not the same, a detailed comparison with these calculations is not valid.

6. Heater

In order to make the probe operational for use in supercooled clouds, a heater has been designed and added so that the original shape of the body remains the same. About 50 cm of nichrome wire is wound around a tapered thread as close to the tip as is possible mechanically. Glyptal paint is used to insulate the wire from the metal, and epoxy is used to cover the wire and fill in the body. The epoxy is then machined to conform to the desired external shape. A temperature control circuit with a thermistor mounted at the rear of the main body was built so that the temperature of the probe could be controlled and monitored. For the Queen Air 56 W of heat is supplied by using 30 gauge nichrome wire. At speeds of 75 m sec^{-1} and ambient temperatures near -30C , the heater can maintain the temperature of the probe at $+25\text{C}$.

Comparative tests in supercooled clouds using a heated and unheated probe have demonstrated that the heater has been effective not only in keeping the orifice from icing but also in preventing malfunctions caused by icing of the electrode.

7. Flight tests and comparison with other instruments

During the past two years large numbers of flights have been made on both the Queen Air and The Explorer using the probe as a research tool. These flights have also served as extensive flight tests for the instrument. As with any new instrument there were problems to be overcome before the instrument could become truly operational. Most of the problems were those typical of airborne electronic instrumentation of high-sensitivity ground loops, radio interference, microphonics, etc. These problems have now been eliminated so that the electrostatic disdrometer has become an

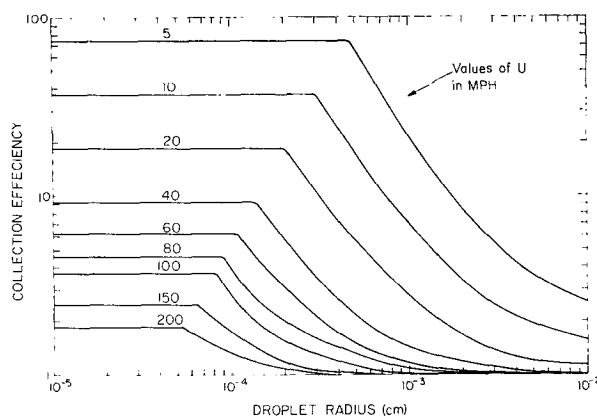


FIG. 10. Theoretically calculated collection efficiency vs particle radius of the electrostatic disdrometer for the aircraft speeds shown.

operational airborne instrument with a high degree of reliability requiring minimal maintenance.

In addition to tests designed to check and eliminate electronic problems, there have been many comparisons made between the electrostatic disdrometer and the Johnson-Williams (J-W)² hot-wire, liquid-water-content meter and droplet replicas obtained from a slide impactor. Before presenting the results of comparisons, it seems appropriate to briefly discuss the other instruments and some of the difficulties with each.

The J-W liquid-water-content meter is a commonly used instrument, which was mounted on the NCAR Queen Air by the NCAR Research Aviation Facility for general use. The quoted time response of the instrument is $\sim 0.6 \text{ sec}$. Proper use requires compensation for different temperatures, pressures and airspeeds. Even when properly compensated, there is baseline drift. After passage through clouds with liquid water contents on the order of 1.0 gm m^{-3} or higher, the instrument frequently gives readings of negative liquid water contents of 0.05 gm m^{-3} . The reference wire inside the instrument housing is probably being wetted during passage through the cloud. Choice of the baseline during data reduction is therefore rather arbitrary and a source of error. Other workers have found that it tends to underestimate the amount of liquid water in a cloud when droplets exceed approximately $30 \mu\text{m}$ in diameter (Owens, 1957; Spyers-Duran, 1968).

The impactor slides used in these comparisons are 4.4 cm long by 1.1 cm wide and are fired in a slide gun with an exposure opening of 3.7 cm. The exposure times are measured for each exposure and average about 12 msec. For the present comparisons the slides were coated with a thin layer of soot similar to the technique used by Squires and Gillespie (1952). Warner (1969) referred to some unpublished work by Squires in which the ratio between the impaction crater diameter and

² Johnson-Williams, Inc., 2300 Leghorn Ave., Mountain View, Calif.

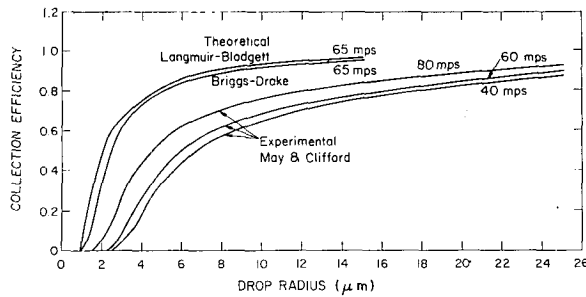


FIG. 11. Theoretically and experimentally determined collection efficiencies vs droplet radius for a slide or ribbon 1.1 cm wide.

the actual droplet diameter for soot was determined for a speed of 65 m sec^{-1} . Squires' flattening ratio has also been used by Auer (1969), and a figure showing this factor as a function of aircraft speed and droplet diameter is given in an unpublished report to the Bureau of Reclamation.

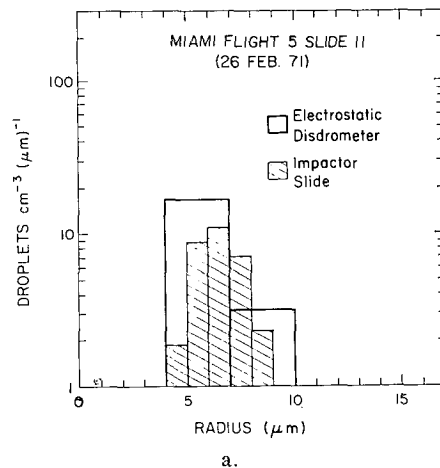
Theoretical collection efficiencies computed for an infinite ribbon by Briggs and Drake at NCAR in some unpublished work are used to correct for droplet loss by flow around the slide. The calculations are similar to those of Langmuir and Blodgett (1946) for ribbons but incorporate improved numerical techniques. These calculations and those of Langmuir and Blodgett are shown in Fig. 11. Recent experimental work with aerosols carried out by May and Clifford (1967) and Starr (1967) and formulated in terms of the Stokes number (the ratio of the stop distance of the particle to the collector dimension) raises some doubt about the theoretically calculated collection efficiencies for impactor slides. The applicability of the experimental results are also uncertain since the experiments were performed with larger particles and lower velocities than those encountered in the case of cloud droplets impacting at aircraft speeds. Also, the calculations are for infinite ribbons, whereas the experimental results are for finite plates. Additional theoretical calculations now being made by Drake using the exact geometry of the slide as it appears when exposed by the gun should yield a better value of the collection efficiency; they will be published later.

In addition to the above problems, there are other difficulties in making detailed comparisons with other instruments. The instruments are mounted at different locations on the aircraft and have different sampling times so that none of them are sampling the same region or volume of the cloud.

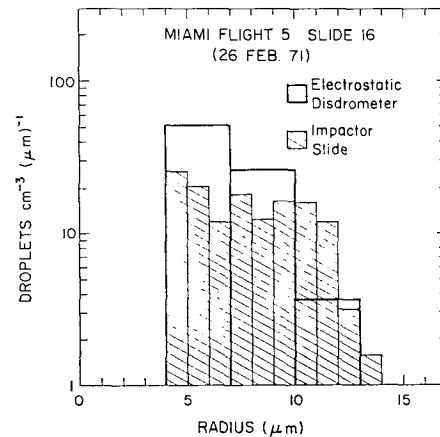
On the Queen Air the electrostatic disdrometer is mounted on the nose about 1 m forward of the windshield on a strut 30 cm high. The J-W hot-wire instrument is mounted under the wing about 25 cm from the skin and 3 m from the fuselage. The slide gun is fired through the top of the fuselage about 1.5 m behind the windshield with slides exposed 20 cm from the skin.

Twelve flights were made in the vicinity of Miami, Fla., from 24 February to 3 March 1971, for comparison of the disdrometer with the J-W instrument and slide impactor in warm clouds in which there could be no problems caused by icing. The flights were made in small non-precipitating cumuli with vertical development seldom greater than 1500 m and cloud top temperatures always warmer than 0C . Because of the quasi-maritime air source for the clouds, the minimum droplet size was usually within the lower limit of the electrostatic disdrometer sizing range. Examples of comparisons are described below. At the time these flights were made, the channel width of the electrostatic disdrometer was $3 \mu\text{m}$ for each channel, so that the range of droplet radii of the first nine channels was from 4 to $31 \mu\text{m}$ with one channel for all droplets $> 31 \mu\text{m}$ in radius.

Figs. 12a and 12b show two separate comparisons of the droplet size distributions as measured by the disdrometer and the impactor slide. It can be seen that



a.



b.

FIG. 12. Two comparisons between droplet size distribution measurements from the electrostatic disdrometer and soot impactor slide replicas: (a) on the edge of a cloud at 1830 m, air temperature = 11.2C ; (b) in the middle of a cloud at 2400 m, air temperature = 7.7C .

agreement between the two is good for both total number of the droplets counted as well as width of the spectrum under quite different conditions. Further comparisons of the total droplet density measured by the disdrometer and the slide are shown in Table 2. Considering uncertainties in collection efficiency for the slide and possible errors in the flattening ratio, agreement is good.

Some of the results of the comparisons of liquid water are shown in Fig. 13. The data from the disdrometer are plotted as a solid line, those from the J-W hot-wire device as a dashed line, and those from the slide as the circled point. Further instantaneous comparisons of the three methods are shown in Table 3. From Table 3 and Fig. 13 it can be seen that the disdrometer data agree more closely with the slide data and that the J-W values are consistently higher than those calculated from the disdrometer data.

The data presented here are representative of other data that have been collected. Of course, there are times when agreement between all three instruments is poor, which is not surprising when problems of mounting location, sampling time, sampling volume, and natural variability of the cloud, indicated by the short-term fluctuation of the droplet spectra, are considered.

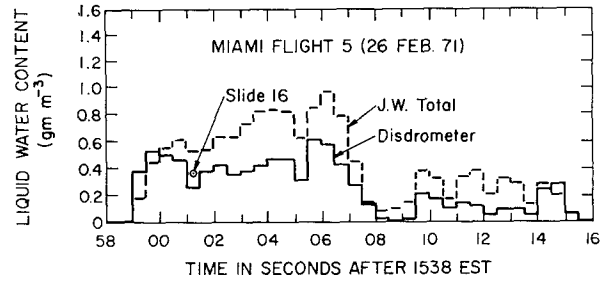


FIG. 13. A comparison between liquid water contents measured at 5980 m by the electrostatic disdrometer, the Johnson-Williams hot-wire device, and an impaction slide.

8. Summary and conclusions

The electrostatic disdrometer, a droplet sizing device based on the original model developed by Keily and Millen (1960) for AFCRL, was tested, modified, and calibrated in our laboratory for use as an automatic, continuous cloud droplet probe on aircraft. Laboratory investigations have shown that soon after entry an incoming droplet is broken into many fragments, the number of which is dependent on drop size. These fragments impact and splash on an electrode raised to a potential of 510 V. A voltage pulse dependent upon

TABLE 2. Comparison between total droplet concentrations measured by the electrostatic disdrometer and impaction slides.

Slide no.	Total droplets per cubic centimeter	
	Electrostatic disdrometer	Slide
26 February 1971		
9	195	67
11	60	36
12	224	169
13	274	197
15	233	229
16	241	140
17	191	66
18	132	144
20	111	111
21	311	152
22	120	152
23	329	394
24	185	417
25	56	216
1 March 1971		
1	196	196
3	425	212
4	154	132
5	86	102
6	296	157
7	133	338
8	205	67
9	185	149
10	175	356
12	139	74
13	223	313
14	244	183
17	282	319
18	115	148
19	126	105
20	130	26

TABLE 3. Comparison between total liquid water contents measurements by the electrostatic disdrometer, Johnson-Williams hot-wire device, and impaction slides.

Slide no.	Total liquid water content (gm m ⁻³)		
	Electrostatic disdrometer	Slide	J-W Hot-wire
26 February 1971			
9	0.25	0.11	0.40
11	0.06	0.04	—
12	0.30	0.28	0.40
13	0.34	0.38	0.33
15	0.21	0.15	0.27
16	0.38	0.36	0.55
17	0.27	0.19	0.40
18	0.18	0.33	0.29
20	0.13	0.12	0.42
21	0.44	0.25	1.00
22	0.12	0.15	0.20
23	0.37	0.46	0.55
24	0.21	0.35	0.25
25	0.04	0.09	—
1 March 1971			
1	0.56	0.70	0.10
3	0.65	0.54	0.90
4	0.17	0.39	0.40
5	0.09	0.11	0.10
6	0.55	0.52	1.00
7	0.18	0.58	0.50
8	0.27	0.08	0.40
9	0.28	0.22	0.50
10	0.21	0.25	0.30
12	0.12	0.21	0.10
13	0.25	0.66	0.70
14	0.35	0.50	0.50
17	0.39	0.60	0.70
18	0.11	0.21	0.10
19	0.13	0.15	0.20
20	0.12	0.17	0.10

droplet size is generated during impaction so that a reproducible calibration curve is obtained. In actual usage, pulses are amplified and fed into a 10-channel pulse-height analyzer that accumulates and reads out the data each 0.5 sec. The range of droplet radii that can be measured by the instrument is $4\ \mu\text{m}$ to about $30\ \mu\text{m}$ with upper limit fixed primarily by the low number density of larger droplets found in clouds.

Airborne tests of the instrument on The Explorer sailplane and an NCAR Queen Air have shown the present instrument to operate reliably with minimal maintenance. Comparisons in warm clouds of the electrostatic disdrometer with the Johnson-Williams hot-wire, liquid-water-content meter and with impaction slide replicas have shown that the disdrometer measurements generally agree quite well with the other methods.

Because of its small size, low power consumption, operational reliability, and automatic operation and analysis of data, the electrostatic disdrometer is of maximum value for the synchronous observation of droplet spectra with other vital cloud physics parameters such as the vertical air speed, temperature and humidity. The principle of operation of the instrument can be readily adapted for measurements in the drizzle and raindrop size range where the mechanical and electronic problems should be less severe than those encountered with the present instrument.

REFERENCES

- Auer, A. A., Jr., 1969: A cloud droplet sampler. An Information Supplement Prepared for the Office of Atmospheric Water Research, U. S. Bureau of Reclamation, 18 pp.
- Colgate, S. A., and J. M. Romero, 1970: Charge versus drop size in an electrified cloud. *J. Geophys. Res.*, **75**, 30, 5873-5881.
- Drake, R. L., W. L. Briggs and T. J. Wright, 1972: Airflow pattern and droplet trajectories about an electrostatic cloud droplet probe. *Pure Appl. Phys.* (in press).
- Harris, W. J., 1964: Device for producing droplet samples of suspensions for electron microscopy and especially for quantitative particle assay. *J. Sci. Instr.*, **41**, 636-637.
- Keily, D. P., 1964: Measurement of drop size distribution and liquid water content in natural clouds. Final rept., Contract AF19(628)-259, for Air Force Cambridge Research Laboratories, Bedford, Mass., 13 pp.
- , and S. G. Millen, 1960: An airborne cloud-drop-size distribution meter. *J. Meteor.*, **17**, 349-356.
- Krasnogorskaya, N. V., 1969: Warm cloud electricity. *Planetary Electrodynamics*, Vol. 1, (S. C. Coroniti and J. Hughes, Eds.), New York, Gordon and Breach, 427-434.
- Langmuir, I., and K. B. Blodgett, 1946: A mathematical investigation of water droplet trajectories. AAF TR5418, Air Material Command, AAF.
- May, K. R., and R. Clifford, 1967: The impaction of aerosol particles on cylinders, spheres, ribbons and discs. *Ann. Occup. Hyg.*, **10**, 83-95.
- Miller, A. H., C. E. Sheldon and W. R. Atkinson, 1965: Spectral study of the luminosity produced during the coalescence of oppositely charged falling water drops. *Phys. Fluids*, **8**, 1921-1928.
- Owens, G. V., 1957: Wind tunnel calibration of three instruments designed for measurement of the liquid water content of clouds. Tech. Note No. 10, Cloud Physics Laboratory, The University of Chicago, 15 pp.
- Spyers-Duran, P. A., 1968: Comparative measurements of cloud liquid water using heated wire and cloud replicating devices. *Proc. Intern. Conf. of Cloud Physics*, Toronto, Canada, 154-158.
- Squires, P., and C. A. Gillespie, 1952: A cloud-droplet sampler for use on an aircraft. *Quart. J. Roy. Meteor. Soc.*, **78**, 387-393.
- Starr, J. R., 1967: Inertial impaction of particulates upon bodies of simple geometry. *Ann. Occup. Hyg.*, **10**, 349-361.
- Warner, J., 1969: The microstructure of cumulus cloud. Part I. General features of the droplet spectrum. *J. Atmos. Sci.*, **26**, 1049-1059.